CLM - P 526

CLM - P 526

UKAEA

Preprint

MULTIDIRECTIONAL INTERFEROMETRY DETERMINATION OF ELECTRON DENSITY PROFILES

A J HAMONIC

CULHAM LABORATORY
Abingdon Oxfordshire

1978

CLM - P526

MULTIDIRECTIONAL INTERFEROMETRY DETERMINATION OF ELECTRON DENSITY PROFILES

By

A. J. Hamonic*
EURATOM/UKAEA Association for Fusion Research,
Culham Laboratory, Abingdon, Oxon, OX 14 3DB, U.K.

ABSTRACT

The technique of deducing plasma density profiles in circularly symmetric plasmas from the Abel inversion of phase shifts measured by a parallel beam multichannel interferometer is generalized to a multidirectional array of beams and to an electron density distribution which can be described by any kind of "sufficiently regular" non-concentric contours, including the quasi-triangular and "D" shapes characterizing certain tokamak plasmas.

(Submitted for publication in Plasma Physics).

*attached from Department of Electrical Engineering, University College, Cork, Ireland.

February 1978

1. INTRODUCTION

Multichannel interferometric determination of the electron density profile is needed on many plasma devices. GORBUNOV et al (1968), (1973), GORBUNOV (1973), GRIBKOV et al (1974), VERON, CERTAIN and CRENN (1975) have used parallel or perpendicular beams for that purpose. But engineering constraints very often do not allow the ideal disposition of windows so that the only data available are interferometric measurements of the phase-shifts introduced by the electron density over a few non-parallel paths. Moreover tokamaks often show displaced elliptic, quasi-triangular or D shapes which cannot easily be dealt with. BAKER (1974) devised a method to determine the density profile in case of elliptic symmetric and asymmetric plasmas with the degree of asymmetry given beforehand. The method amounts to constructing that density profile for which the Abel integral most closely matches the experimental phase shift data. In this paper we consider first symmetric and asymmetric circular density profiles and show how to reduce computational operations to a minimum using Cavalieri's Principle (HALMOS (1950)), then go to deal with any kind of sufficiently regular displaced profiles.

2. CIRCULAR CASE. APPLICATION OF CAVALIERI'S PRINCIPLE

Let us assume that the deviation of the ray from a straight line is negligible. For a beam with off-centre distance x (Fig. 1), the phase difference of a wave probing a plasma between A_1 and A_2 will be

$$\psi(x) = \frac{1}{2\lambda\, n_c} \int_{y_1}^{y_2} n(r)\, dy \qquad (1)$$

where $n(r)$ is the radial electron density profile

λ wavelength of the probing beam

n_c cut-off density for the wavelength λ.

In the absence of axial symmetry, we shall consider the lines of constant density as being defined by a family of off-centred circles. The equation for each circle is

$$(x - \Delta(r))^2 + y^2 = r^2 \qquad (0 \leq r \leq a) \tag{2}$$

with "a" the radius of the circular plasma. Following GORBUNOV et al (1968), GORBUNOV (1973), $\Delta(r)$ is the displacement of the circumcircle of radius r along the displacement axis x, relative to the centre of the boundary surface with r = a.

Let us consider the displaced surfaces and probe the plasma along the P direction (Fig. 2(a)) with

$$\Delta(r) = x_o(1 - \frac{r}{a})$$

$$x_n = \Delta(r_n) \quad .$$

The direct evaluation of the integral (1) is difficult. However the application of Cavalieri's Principle, as described in Appendix I, demonstrates that the integral is unchanged if instead of the configuration shown in Fig. 2(a) we consider the family of displaced circles centred on the x'_n instead of the x_n with $x_n = x'_n \cos\gamma$ (Fig 2(b)).

A particular case of this property is the invariance of the integral when probing parallel to the displacement axis. In that case, it is impossible to detect any shift of the centre of the plasma column, GORBUNOV et al (1968).

The integral (1) is readily calculated using

$$R = \frac{r}{a} \quad , \quad X_o = \frac{x_o}{a} \quad , \quad X_n = \Delta(R_n) \quad , \quad X'_n = X_n \cos\gamma \quad , \quad N(R) = \frac{n(R)}{n(0)} \quad .$$

With the off-centre distance of the probing path and δ defined as on Fig 2(b), we have

$$\psi(D,\delta) = -\frac{n(o)a}{\lambda n_c}\int_{\tilde{R}(D)}^{1}\sqrt{R^2(1-X'^2_o) - 2RX'_o(D-X'_o) - (D-X'_o)^2}\,N'(R)\,dR$$

$\tilde{R}(D)$ is the radius of the circle tangent to the probing line P, that is

$$\tilde{R}(D) = \frac{D - X'_o}{1 - X'_o}$$

if $$D - X'_o \geq 0 \ ,$$

and $$\tilde{R}(D) = -\frac{D - X'_o}{1 + X'_o}$$

if $$D - X'_o \leq 0 \ .$$

Let us consider a set of measurements defined by the two parameters D and δ, and at each of these measurements, let us associate a positive integer I $[\psi(L)]$. To each of these measurements corresponds a value $\tilde{R}(D_L) = R_L$. Then, if we consider M displaced circles of radius R_L, $1 \leq L \leq M$, and a linear approximation of the density between the different circles, we obtain

$$N'(R_J) = \frac{N(R_{J+1}) - N(R_J)}{R_{J+1} - R_J}$$

with $$R_{J+1} \neq R_J$$

and

$$\psi(L) = -\frac{n(o)a}{\lambda n_c}\sum_{J=L}^{M-1}\int_{R_J}^{R_{J+1}}\sqrt{R^2(1-X'^2_{oL}) - 2RX'_{oL}(D_L-X'_{oL}) - (D_L-X'_{oL})^2}\,N'(R_J)dR$$

$$\psi(L) = -\frac{n(o)a}{\lambda n_c}\sum_{J=L}^{M-1}\frac{N(R_{J+1}) - N(R_J)}{R_{J+1} - R_J}\int_{R_J}^{R_{J+1}}\sqrt{R^2(1-X'^2_{oL}) - 2RX'_{oL}(D - X'_{oL}) - (D_L-X'_{oL})^2}\,dR \ .$$

Defining

$$U^{L}_{J,J+1} = \int_{R_J}^{R_{J+1}} \sqrt{R^2(1-X'^{2}_{oL}) - 2RX'_{oL}(D_L - X'_{oL}) - (D_L - X'_{oL})^2}\; dR$$

and

$$V_J^{L} = \frac{U^{L}_{J-1\,J}}{R_J - R_{J-1}} - \frac{U^{L}_{J\,J+1}}{R_{J+1} - R_J}$$

we obtain

$$-\psi(1)\frac{\lambda n_c}{n(o)a} = -N(R_1)\frac{U^{1}_{1,2}}{R_2-R_1} + N(R_2)V_2^{1} + N(R_3)V_3^{1} + \ldots + N(R_{M-2})V^{1}_{M-2} + N(R_{M-1})V^{1}_{M-1} + N(R_M)\frac{U^{1}_{M-1,M}}{R_M - R_{M-1}}$$

$$-\psi(2)\frac{\lambda n_c}{n(o)a} = -N(R_2)\frac{U^{2}_{2,3}}{R_3-R_2} + N(R_3)V_3^{2} + \ldots N(R_M)\frac{U^{2}_{M-1,M}}{R_M - R_{M-1}}$$

$$\psi(M-2)\frac{\lambda n_c}{n(o)a} = -N(R_{M-2})\frac{U^{M-2}_{M-2,M-1}}{R_{M-1} - R_{M-2}} + N(R_{M-1})V^{M-2}_{M-1} + N(R_M)\frac{U^{M-2}_{M-1,M}}{R_M - R_{M-1}}$$

$$-\psi(M-1)\frac{\lambda n_c}{n(o)a} = -N(R_{M-1})\frac{U^{M-1}_{M-1,M}}{R_M - R_{M-1}} + N(R_M)\frac{U^{M-1}_{M-1,M}}{R_M - R_{M-1}}$$

$$-\psi(M)\frac{\lambda n_c}{n(o)a} = 0 = N(R_M)$$

which can be written

$$(T)\quad \begin{bmatrix} N(R_1) \\ N(R_2) \\ \\ N(R_{M-2}) \\ N(R_{M-1}) \\ N(R_M) \end{bmatrix} = \begin{bmatrix} -\psi(1)\frac{\lambda n_c}{n(o)a} \\ -\psi(2)\frac{\lambda n_c}{n(o)a} \\ \\ -\psi(M-2)\frac{\lambda n_c}{n(o)a} \\ -\psi(M-1)\frac{\lambda n_c}{n(o)a} \\ -\psi(M) = 0 \end{bmatrix}$$

and, if (T^{-1}) exists

$$\begin{bmatrix} n(R_1) \\ n(R_2) \\ n(R_{M-1}) \\ n(R_M) \end{bmatrix} = (T^{-1}) \begin{bmatrix} -\psi(1)\frac{\lambda n_c}{a} \\ -\psi(2)\frac{\lambda n_c}{a} \\ -\psi(M-1)\frac{\lambda n_c}{a} \\ -\psi(M)\frac{\lambda n_c}{a} = 0 \end{bmatrix}$$

$n(R_i)$ being the calculated electron density as a function of the radi of the displaced circles.

Computational trials of the method have been made with 14 beams taking into account the limited access on a machine like RFX. A linear approximation such as the above with a density profile of $\frac{N(R)}{N(o)} = \frac{1}{2}(1 + \cos \pi R^{\varepsilon})$ with $\varepsilon = 1.5$, 3 and subsequently a hollow profile

$$\frac{N(R)}{N(o)} = 1 + \tfrac{1}{2}(\cos \pi R^2 - \cos \pi R) - R^2 \quad \text{were assumed.}$$

The profile has been reconstructed, first with no displacement of the column (symmetric case) then some given displacement (asymmetric case).

Fig. 3, 4 and 5 show respectively a representation of the assumed electron density profile where the density is plotted as a function of the radius R of the displaced circles (contours of equal density) as well as the reconstructed profile representation in the case $\varepsilon = 1.5$, 3 and hollow profile with different parameters X_o and θ.

Fig. 6, 7 and 8 show respectively the assumed normalized electron density profile given on the displacement axis and the respective recalculated points in the cases $\varepsilon = 1.5$, 3 and hollow profile.

These graphs serve to illustrate the accuracy of the method which enables us to recalculate a density profile which exhibits a high degree of asymmetry $X_o = 0.8$ as well as a hollow shape. The absolute error ΔN in the finding of the density profile in the case of the Fig. 3 with $X_o = 0$ is less than $1.65\ 10^{13}\ cm^{-3}$ for all the cords probed. See Table 1.

TABLE 1 Displaced Circles Case $N(R)/N(0) = \frac{1}{2}(1 + \cos \pi R^{1.5})$

Normalized circles radii	Given density (cm^{-3})		Calculated density (cm^{-3})		Absolute error (cm^{-3})	
0.000	6.6	10^{14}	6.690	10^{14}	9	10^{12}
0.217	6.436	"	6.480	"	4.4	10^{12}
0.233	6.395	"	6.460	"	6.5	10^{12}
0.250	6.349	"	6.458	"	1.1	10^{13}
0.450	5.224	"	5.224	"	0.00	
0.483	4.926	"	4.975	"	4.9	10^{12}
0.650	3.051	"	3.055	"	4.	10^{11}
0.833	8.893	10^{13}	7.239	10^{13}	1.65	10^{13}
1.000	0.000		0.000		0.00	

Similar results hold for all the other cases ($\varepsilon = 3$ and hollow profile). The principal limitation of the method appears to be the degree to which a profile consisting of displaced circles accurately models the true electron density distribution. To overcome this limitaion a more general method capable of dealing with elliptical, quasi-triangular, and D-shaped profiles has been developed.

3. GENERAL METHOD

a) Mathematical developments

Let us now take (1) with a slight change, i.e., r is now a parameter defining each of the equi-density curves. (It has been the radius of the equi-density circles and we shall see later that it can be the major axis of ellipses.)

If the equation of the equi-density curves can be written as $f(y,x,r) = 0$ or more specifically

$$a(x,r)y^2 + b(x,r)y + c(x,r) = 0 \qquad (3)$$

and if $\frac{dy}{dr}$ exists, (1) can be rewritten as

$$\psi(x) = \frac{1}{2\lambda n_c} \int_{r(y_1)}^{r(y_2)} n(r) \frac{dy}{dr} \, dr , \qquad (4)$$

The probing path intersects one of the equi-density curves at only one tangent point. Let the value of the parameter r be r_0 at that point.

We can write ψ as

$$\psi(x) = \frac{1}{2\lambda n_c} \left[\int_{r_1}^{r_0} n(r) \frac{dy_-}{dr} \, dr + \int_{r_0}^{r_2} n(r) \frac{dy_+}{dr} \, dr \right]$$

where y_- and y_+ are solutions of the equation (3).

Again

$$2\lambda n_c \, \psi(x) = n(r)y_-(r) \Big|_{r_1}^{r_0} - \int_{r_1}^{r_0} n'(r)y_- dr$$

$$+ n(r)y_+(r) \Big|_{r_0}^{r_2} - \int_{r_0}^{r_2} n'(r)y_+ dr ,$$

As $n(r_1) = n(r_2) = 0$

(Density nil on the outside curve) and

$y_- (r_0) = y_+ (r_0)$, we obtain

$$2\lambda n_c \, \psi(x) = \int_{r_0}^{r_1} n'(r)y_- \, dr - \int_{r_0}^{r_1} n'(r)y_+ \, dr$$

r_1 and r_2 are equal as they both refer to the same external equi-density curve.

Then

$$2\lambda n_c \, \psi(x) = \int_{r_0}^{r_1} n'(r) \left[y_- - y_+ \right] dr$$

$$= -\int_{r_0}^{r_1} n'(r) \frac{(b^2(x,r) - 4a(x,r)\, c(x,r))^{\frac{1}{2}}}{a(x,r)} \qquad (5)$$

Equation (5) can be used to write a system of linear equations. Taking a linear approximation of the density between the different equi-density curves tangent to the probing paths, we obtain

$$\psi(L) = -d \sum_{J=L}^{M-1} \frac{N(R_{J+1}) - N(R_J)}{R_{J+1} - R_J} \quad X$$

$$X \int_{R_J}^{R_J + 1} \frac{(b^2(X_L,R) - 4\, a(X_L,R)\; c(X_L,R))^{\frac{1}{2}}}{a(X_L, R)} \, dR$$

where d is a normalization factor, N, R the normalized electron density and curve parameter and X_L the normalized off-axis distance of the L^{th} probing path.

b) Particular case. Displaced ellipses.

Let us consider a family of displaced ellipses. There are three important axes (Fig. 9).

The probing axis P, defined by δ_L and X_L.

The displacement axis A, defined by η.

The inclination axis I (Major axis of the ellipses) defined by β. Let us define a system of co-ordinates in which the X' axis is parallel to the I axis and Y' is perpendicular to it. The equation for the ellipses is

$$\left[X' - \Delta_{x'}(R)\right]^2 + \alpha^2(R)\left[Y' - \Delta_{y'}(R)\right]^2 = R^2$$

with $\cos(\eta - \beta) = \Delta_{x'}(R) / \Delta(R)$

$\sin \sin(\eta - \beta) = \Delta_{y'}(R) / \Delta(R)$.

$\Delta(R) = X_0(1 - R)$ is the displacement of the centre of the ellipses of normalized major exis R relative to the external equi-density curve centre.

$\alpha(R) = 1 + \alpha_0(1 - R)$ is the eccentricity of the ellipse of normalized axis R. Note that the eccentricity is a function of R such as to match the circular external section with assumed density 0.

Let us consider a new system of co-ordinates with the Y axis parallel to the probing axis and the X axis perpendicular to it.

The equation of the ellipses relative to the new system of co-ordinates is

$$[X \cos(\delta - \beta) - Y \sin(\delta - \beta) - \Delta(R) \cos(\eta - \beta)]^2$$
$$+ \alpha^2(R) [X \sin(\delta - \beta) + Y \cos(\delta - \beta) - \Delta(R) \sin(\eta - \beta)]^2 = R^2$$

which can be written as

$$a(X,R)Y^2 + b(X,R)Y + c(X,R) = 0$$

with

$$a(X,R) = \sin^2(\delta - \beta) + \alpha^2(R) \cos^2(\delta - \beta)$$

$$b(X,R) = 2[\sin(\delta - \beta)\Delta(R) \cos(\eta - \beta)$$
$$+ \alpha^2(R) X \sin(\delta - \beta) \cos(\delta - \beta)$$
$$- \alpha^2(R) \cos(\delta - \beta)\Delta(R) \sin(\eta - \beta)$$
$$- X \cos(\delta - \beta) \sin(\delta - \beta)]$$

$$c(X,R) = X^2[\cos^2(\delta - \beta) + \alpha^2(R) \sin^2(\delta - \beta)]$$
$$- 2X[\cos(\delta - \beta)\Delta(R) \cos(\eta - \beta) + \alpha^2(R) \sin(\delta - \beta)\Delta(R) \sin(\eta - \beta)]$$
$$- \Delta^2(R) [\cos^2(\eta - \beta) + \alpha^2(R) \sin^2(\eta - \beta)]$$
$$- R^2.$$

The radius of the tangent ellipses to the probing paths is given by

$b^2 - 4ac = 0$ thus,

$$\alpha^2(R) \Delta^2(R) G^2 - 2\Delta(R) X \alpha^2(R) G + X^2 \alpha^2(R)$$
$$- R^2[\sin^2(\delta - \beta) + \alpha^2(R) \cos^2(\delta - \beta)] = 0$$

with

$$G = \sin(\eta - \beta) \sin(\delta - \beta) + \cos(\eta - \beta) \cos(\delta - \beta)$$

and $|X|$ is the probing path off-axis distance.

We have computed the solution of such a problem in the case of maximum eccentricity 2, which is $\alpha_0 = 1$, and maximum displacement $X_0 = 0.4$.

Fig. 10 shows the plasma model with ellipses tangent to the 14 probing paths considered.

As in §1 an electron density profile of the form

$$N(R) / N(0) = \tfrac{1}{2} (1 + \cos \pi R^{1.5})$$

with

$$N(0) = 6.6\ 10^{14}\ cm^{-3}$$

has been assumed, and the profile has then been reconstructed computationally from values of the phase-shifts which would be obtained along the probing paths. As before, in the case of displaced circles, the absolute error is very small indeed and less than $2.1\ 10^{12}\ cm^{-3}$ for all the points but the most external chord, i.e. R = 0.89.

Again we stress here the great accuracy of the method which is able to produce a two dimensional density profile although the probing directions are distributed over 2π, depending of the availability of ports for diagnostic access.

The main drawback of this method is, its high sensitivity to errors in the experimental data.

In order to illustrate this sensitivity, we have introduced a random error of a few % in the phase-shift test set and show on the Fig. 11 the influence of this error on the computed profile.

The curve (a) is the original profile

(b) is the one obtained when no error has been introduced in the phase-shift

(c) is for a random error of a maximum of 1%

(d) is for a random error of a maximum of 2%

(e) is for a random error of a maximum of 4%.

When a random error of more than 4% is introduced, the spurious ringing observed in the calculated results reaches such an amplitude as to render them useless.

TABLE 2 Displaced ellipses case

$$N(R) / N(0) = \tfrac{1}{2}(1 + \cos \pi R^{1.5})$$

Normalized Major Axis	Given Density (cm^{-3})		Calculated Density (cm^{-3})		Absolute Error (cm^{-3})	
0.062	6.596	10^{14}	6.586	10^{14}	1.03	10^{12}
0.112	6.577	"	6.589	"	1.18	"
0.196	6.479	"	6.486	"	0.78	"
0.280	6.249	"	6.264	"	1.54	"
0.363	5.853	"	5.861	"	0.79	"
0.429	5.395	"	5.397	"	0.21	"
0.480	4.955	"	4.951	"	0.41	"
0.516	4.609	"	4.620	"	1.10	"
0.572	3.990	"	3.992	"	0.21	"
0.639	3.193	"	3.184	"	0.84	"
0.661	2.910	"	2.907	"	0.31	"
0.742	1.907	"	1.900	"	0.71	"
0.777	1.486	"	1.465	"	2.10	"
0.887	4.286	10^{13}	3.411	10^{13}	8.76	"
1.000	0.000		0.000		0.00	

CONCLUSIONS

It is well-known that the radial electron density profile in a plasma where the contours of constant density are concentric circles can be deduced by Abel inversion of phase shifts measured in a parallel beam multichannel interferometer.

This paper has used Cavalieri's Principle from the mathematical theory of sets to deal with multi-directional multichannel interferometer and density contours which are non-concentric circles. Furthermore it was demonstrated that the method can be generalized to cater for density contours such as concentric and non-concentric ellipses, and finally any "sufficiently regular" non-concentric contours. The technique is accordingly applicable to the quasi-triangular and "D" shaped plasmas characterizing certain tokamak configurations.

As an example, the case of 14 randomly directed beams probing an electron density distribution defined by a set of contours consisting of mutually displaced ellipses was discussed, and the sensitivity of the reconstructed profiles to random measurement errors was investigated. It was shown in this case that random errors in phase shift measurements of less than 4% could be tolerated.

ACKNOWLEDGEMENTS

The author expresses his appreciation for helpful discussions to Drs. A. K. Seda, A. A. Newton, D. E. Evans and Professor M. C. Sexton.

References

BAKER, K (1974) IPP 2/227

GORBUNOV, E. P. (1973) Plasma Diagnostics, 3, 358.

GORBUNOV, E. P., ERMALOV, I. P. and PLOSKIREV, G. N. (1973) Plasma Diagnostics, 3rd edition, Atomizdat, Moscow, 375.

GORBUNOV, E. P. DNESTROVSKI, Yu N, KOSTOMAROV, D. P., MUL'CHENKO, B. F. (1968) Plasma Diagnostics, M. Atomizdat No. 2, 188.

GRIBKOV, V. A. , ISAKOV, A. I., KALACHEV, N. V., KROKHIN, O. N. and SKLIZKOV, G. V. (1974) Sov. J. Quant. Electron. 4, No. 2, 203

HALMOS, P. R. (1950) "Measure Theory" D. Van Nostrand Company Inc.

VERON, D., CERTAIN, J., CRENN, J. P., (1975) Euratom - CEA Association, Fontenay-aux-Roses, Report EUR-CEA-FC-799.

APPENDIX I

"The integral (1) is unchanged per transformation which shifts the contours of equal density parallelly to the probing direction, provided that the function N(R) stays defined on $[-1, +1]$."

The demonstration of this fact is a simple application of CAVALIERI'S Principle (P R HALMOS (1950)). If X and Y are two sets, the Cartesian product XxY is the set of all ordered points (x,y) where $x \in X$, $y \in Y$

$$XxY = \left\{ (x,y) \quad ; \quad x \in X, y \in Y \right\} .$$

If E is any subset of XxY and x any point of X, we shall call the set $E_x = \left\{ y \quad ; \quad (x,y) \in E \right\}$ the section of E determined by x.
Similarly E^y is defined by

$$E^y = \{x; \ (x,y) \in E\} .$$

Let ν be the Lebesgue measure on X and Y,

If E and F are measurable subsets of X x Y, such that $\nu(E_x) = \nu(F_x)$ for almost every x in X, then $\lambda(E) = \lambda(F)$, where $\lambda = \nu \times \nu$.

In our case, X x Y = R x R; ν is the length, λ is the surface.

E is the set shown on fig. I-1, F on fig. I-2

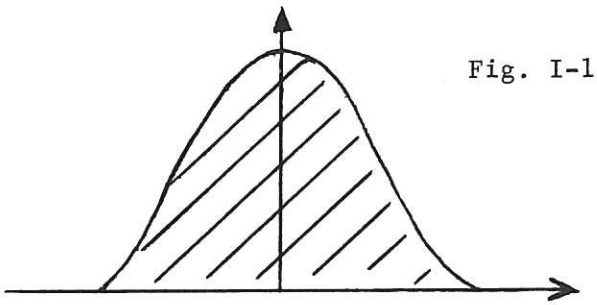

Fig. I-1

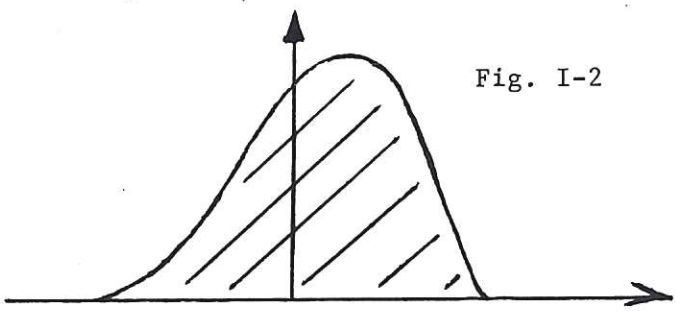

Fig. I-2

As the equi-density contours are shifted, the conditions of the CAVALIERI's principle are fulfilled, and the value of the integral is unchanged per translation of the circles.

APPENDIX II

Calculation of $U^{L}_{J,J+1}$ =

$$\int_{R_J}^{R_{J+1}} \sqrt{R^2(1-X'^2_{OL})-2RX'_{OL}(D_L-X'_{OL})-(D_L-X'_{OL})^2}\,dR$$

$$= \frac{(1-X'^2_{OL})R_{J+1}-X'_{OL}(D_L-X'_{OL})}{2(1-X'^2_{OL})} \sqrt{R^2_{J+1}(1-X'^2_{OL})-2R_{J+1}X'_{OL}(D_L-X'_{OL})-(D_L-X'_{OL})^2}$$

$$- \frac{(1-X'^2_{OL})R_J-X'_{OL}(D_L-X'_{OL})}{2(1-X'^2_{OL})} \sqrt{R^2_J(1-X'^2_{OL})-2R_JX'_{OL}(D_L-X'_{OL})-(D_L-X'_{OL})^2}$$

$$- \frac{(D_L-X'_{OL})^2}{2(1-X'^2_{OL})^{3/2}} \ln$$

$$\left\{ \frac{\sqrt{(1-X'_{OL})^2\{R^2_{J+1}(1-X'^2_{OL})-2R_{J+1}X'_{OL}(D_L-X'_{OL})-(D_L-X'_{OL})^2\}} + (L-X'^2_{OL})R_{J+1} - X'_{OL}(D_L-X'_{OL})}{\sqrt{(1-X'_{OL})^2\{R^2_J(1-X'^2_{OL})-2R_JX'^2_{OL})-2R_JX'_{OL}(D_L-X'_{OL})-(D_L-X'_{OL})^2\}} + (1-X'^2_{OL})R_J-X'_{OL}(D_L-X'_{OL})} \right\}$$

$$= U^{L}_{J,J+1}$$

{T} function of $\tilde{R}(D)$ function of X_o, $\gamma = \delta-\theta$

X_o and θ unknown

D and δ given.

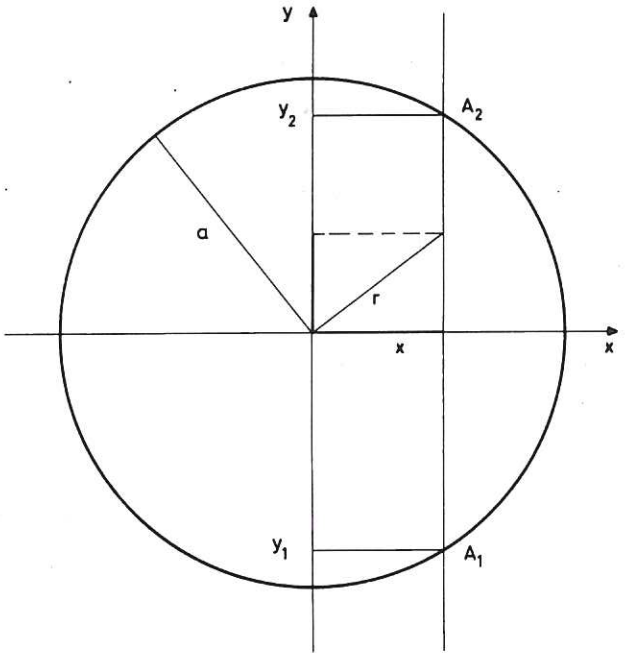

Fig.1 For a beam with off-centre distance x, the phase difference of a wave probing the plasma between A_1 and A_2 is:

$$\psi(x) = \frac{1}{2\lambda n_c} \int_{y_1}^{y_2} n(r)dy \ .$$

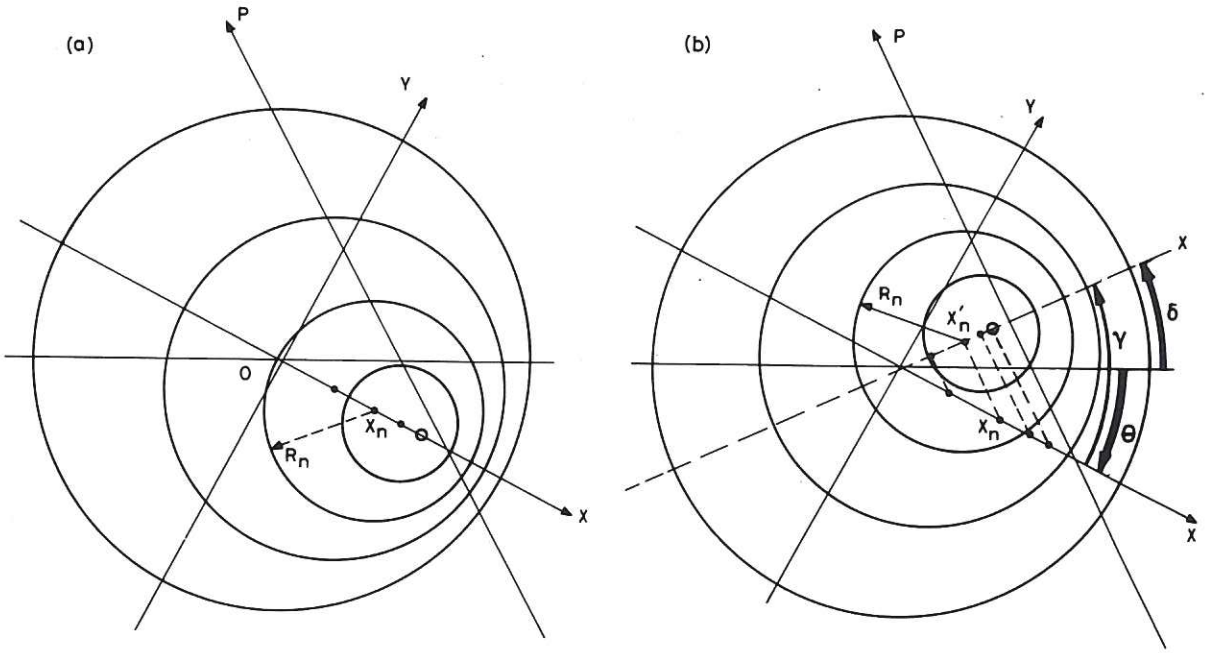

Fig.2 Section of the plasma column showing the displaced circles structure. P is the probing direction. OX is the displacement axis. The integral $\int_{y_1}^{y_2} n(r)dy$, along P is unchanged per translation of the circles from the configuration (a) to the configuration (b).

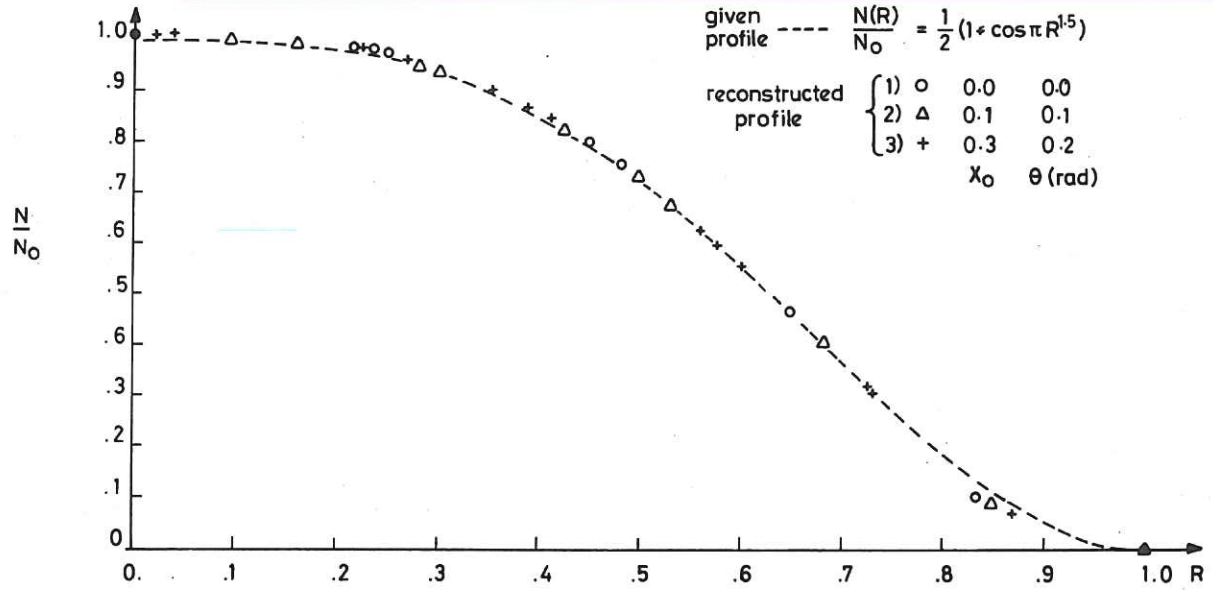

Fig.3 Representation of the electron density profile as a function of the radius of the circles – contours of equal density – for $\epsilon = 1.5$.

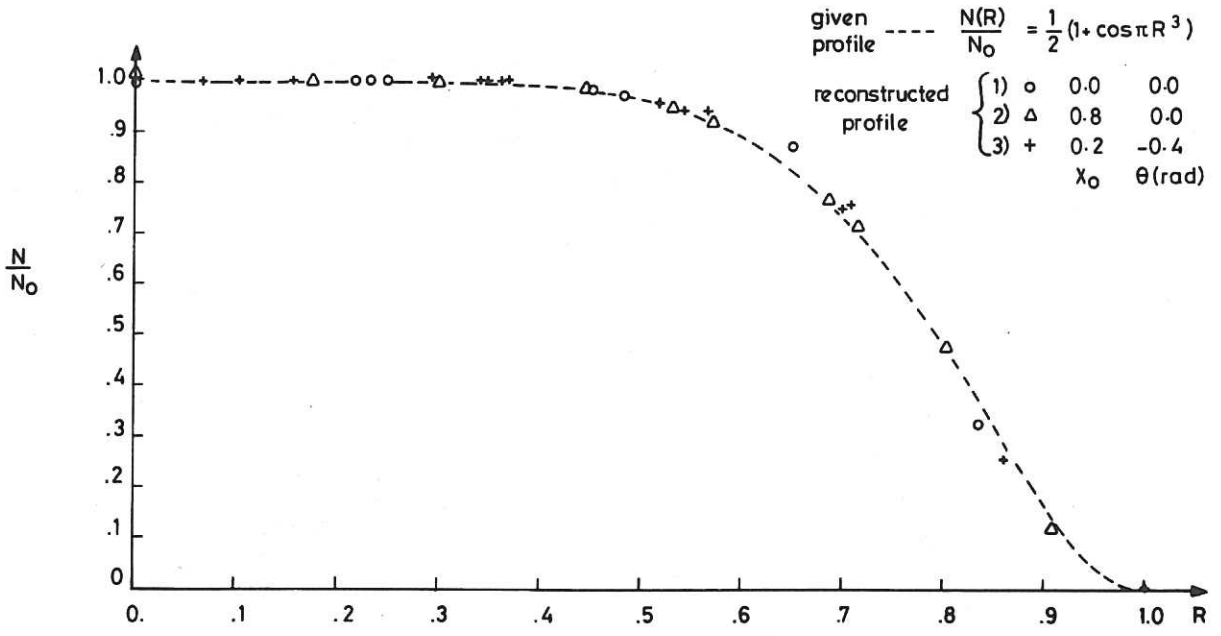

Fig.4 Representation of the electron density profile as a function of the radius of the circles – contours of equal density – for $\epsilon = 3$.

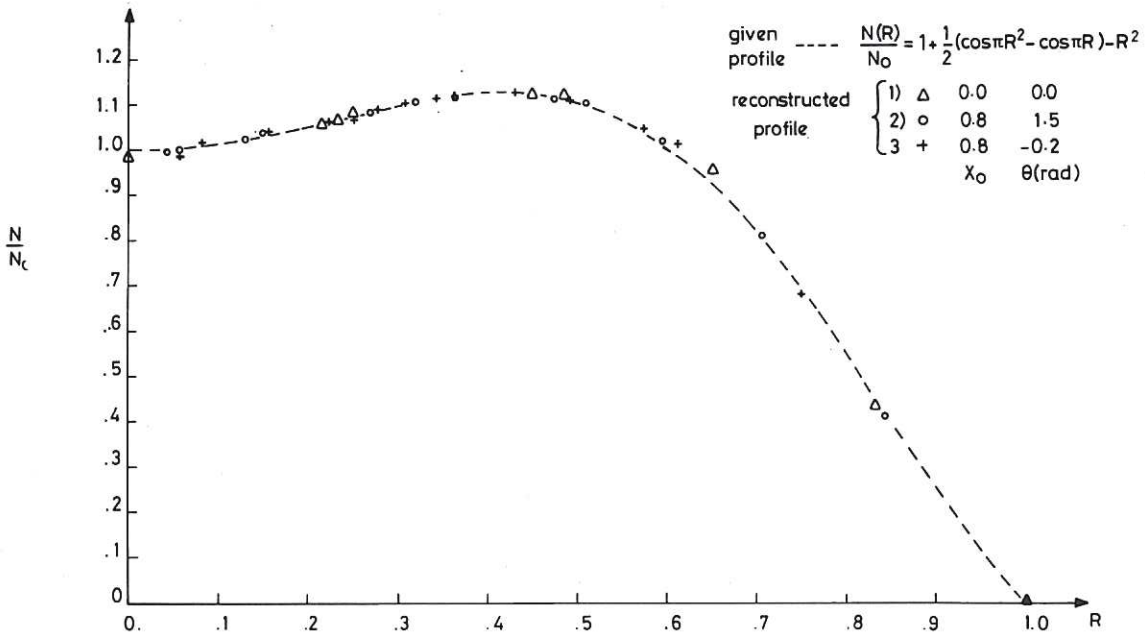

Fig.5 Representation of the electron density profile as a function of the radius of the circles – contours of equal density – for a hollow profile.

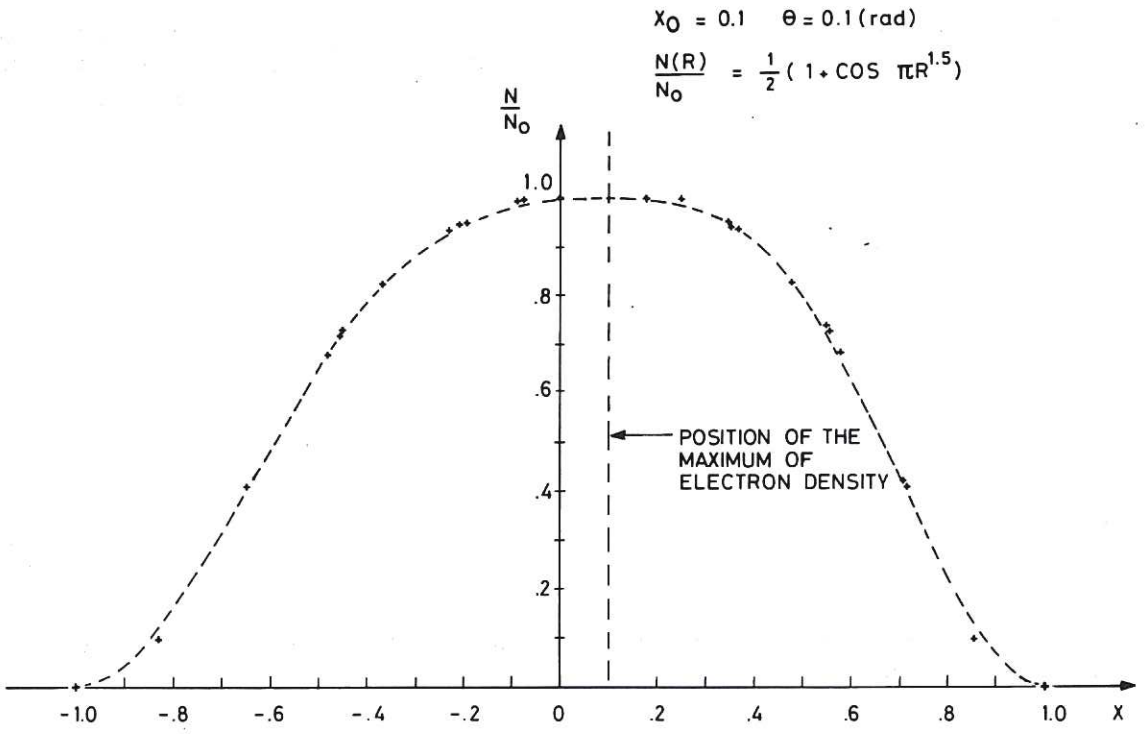

Fig.6 Electron density profile on the displacement axis (Corresponds to the case (2) of the Fig.3).

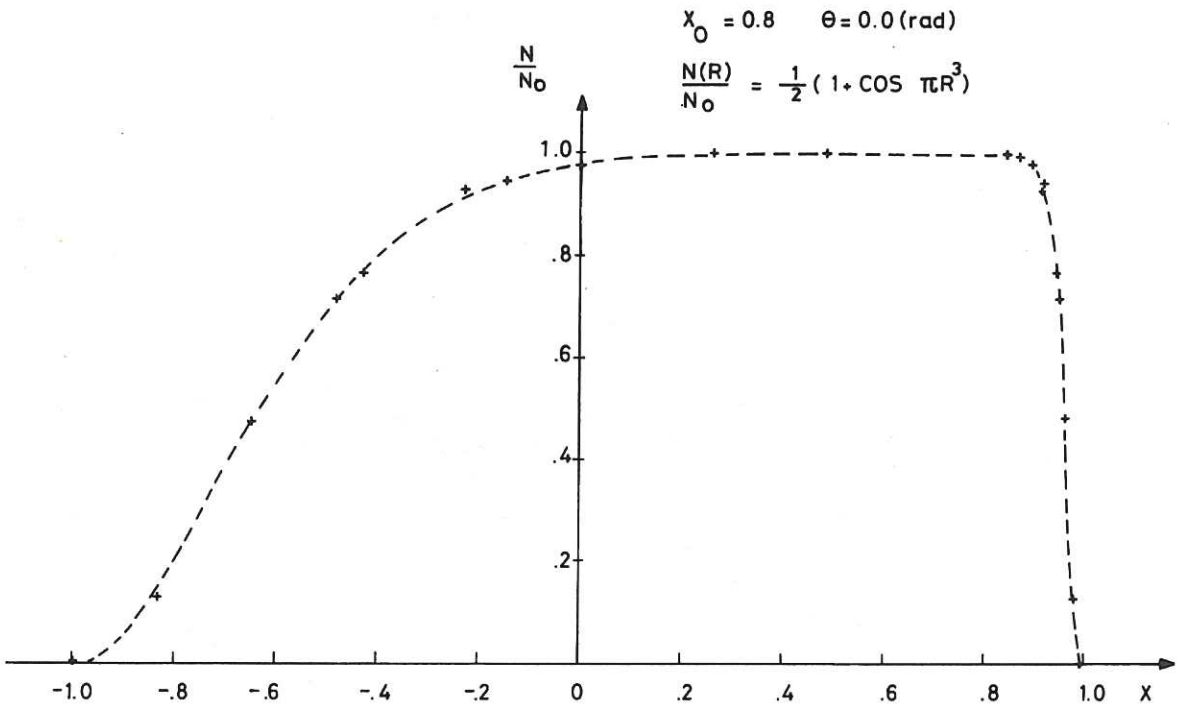

Fig.7 Electron density profile on the displacement axis (Corresponds to the case (2) of the Fig.4).

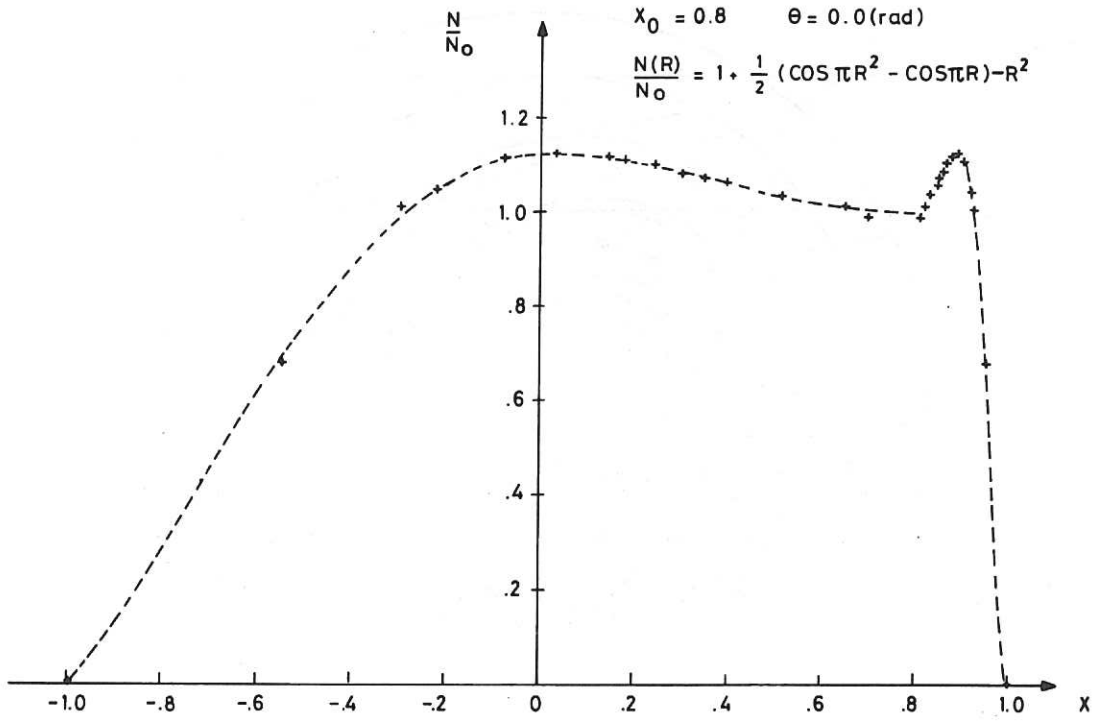

Fig.8 Electron density profile on the displacement axis (Corresponds to the case (3) of the Fig.5).

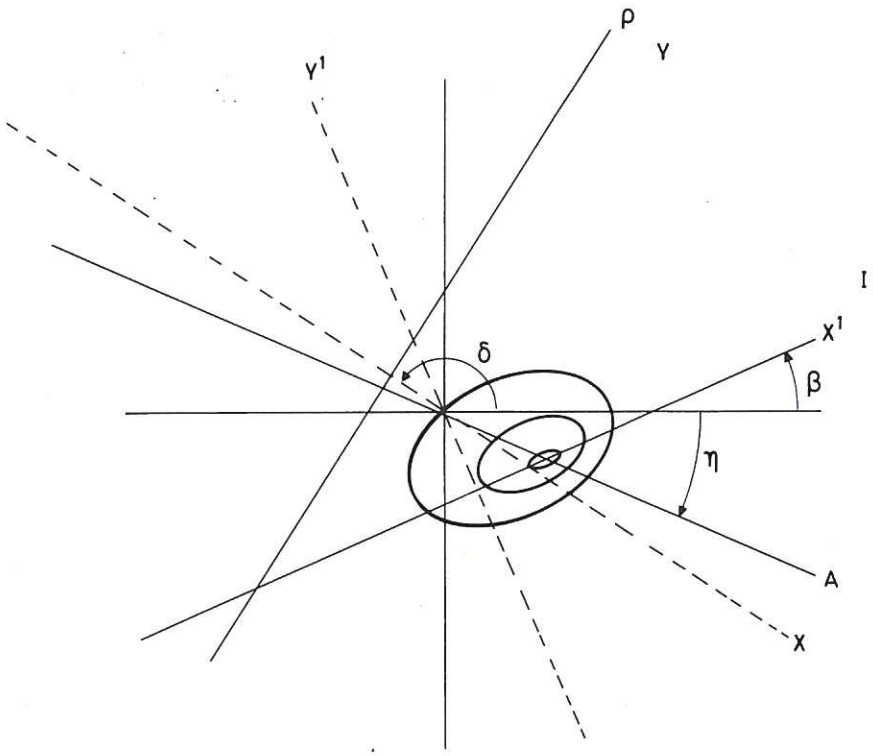

Fig.9 Ellipse model. Definition of the different parameters.

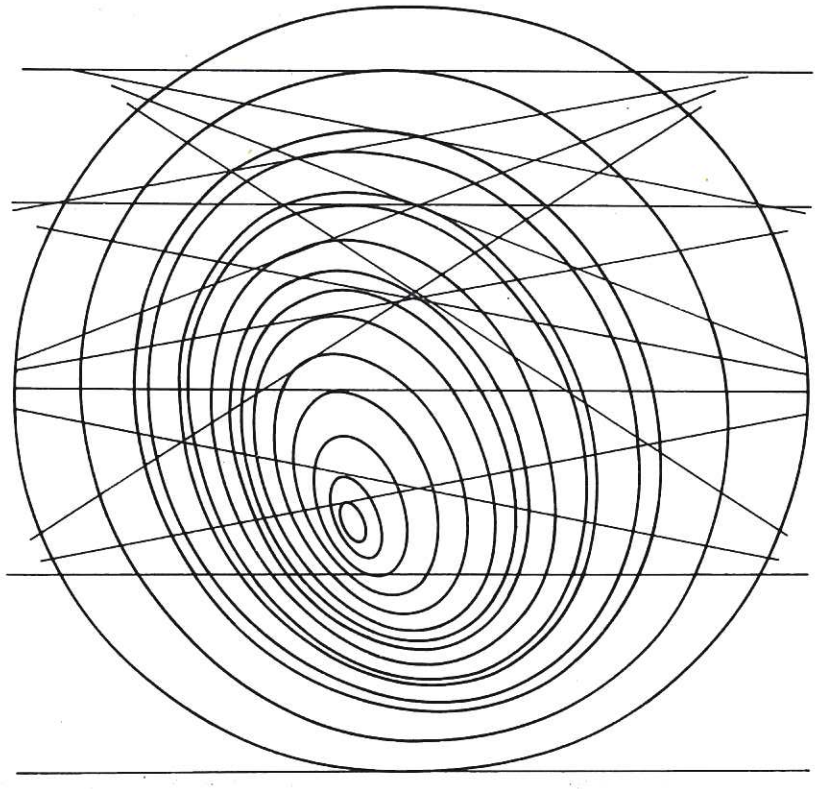

Fig.10 Cross section of the plasma showing the different ellipses tangent to the probing paths. Here $X_0 = 0.4, \beta = 0.39, \eta = -0.39$.

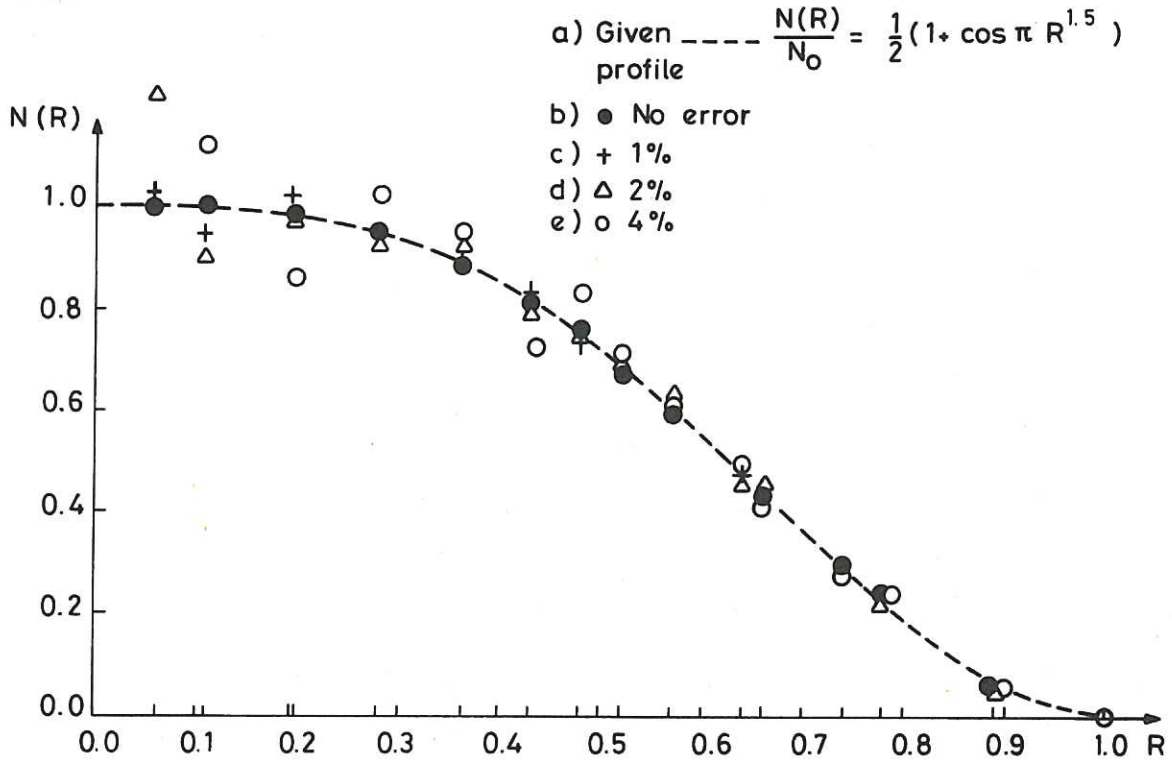

Fig.11 Representation of the electron density profile as a function of the major axis of the ellipses for $\alpha_0 = 1.5, X_0 = 0.4, \beta = 0.39, \eta = -0.39$ and different values of random error.